

Surface Roughness and Residual Stresses on the Fatigue Life of Shot Peened Components: Theoretical Determination

José Solís Romero¹, Alfonso Anguiano García¹, Antonio García Macedo²

¹Instituto Tecnológico de Tlalnepantla. Departamento de Ingeniería Mecánica
División de Estudios de Posgrado e Investigación
josesolis@itesm.mx, ponchito_jr@latinmail.com

²Instituto Tecnológico y de Estudios Superiores de Monterrey-CEM-DIA
Departamento de Ingeniería Mecánica.
josegarc@itesm.mx

Abstract

The effects of the shot peening process on the fatigue damage are analysed and modelled. Surface roughness is modelled in a way that would increase the far-field stress. Compressive residual stresses translated as closure stresses which tend to reduce the application of the far-field stress by introducing this closure stress on the crack flanks and thus the propagation of the crack is expected to be somewhat reduced compared to the unpeened condition.

Resumen

Se analizaron y modelaron matemáticamente los efectos del proceso de granallado que tienen en el daño por fatiga de materiales metálicos policristalinos. La rugosidad superficial se modeló de tal forma que incrementa el esfuerzo aplicado. Los esfuerzos residuales compresivos se convirtieron en esfuerzos de cerradura los cuales tienden a contrarrestar el esfuerzo aplicado dado que el esfuerzo de cerradura actúa en las caras de la grieta reduciendo la velocidad de propagación en comparación con aquellos componentes sin la aplicación del granallado.

Keywords:

Controlled shot peening; fatigue life improvement; micromechanical model.

Palabra claves:

Shot peening controlado; vida en fatiga; modelo micromecánico.

Introduction

For many years controlled shot peening (CSP) was considered as a surface treatment of questionable benefits. This impression was fuelled by contradictory results from fatigue experiments [1,2]. It is now clear that the performance of CSP in terms of fatigue, depends on the balance between its beneficial (compressive residual stress and work hardening) and detrimental effects (surface roughening) [3,4]. Hence, in order to achieve a favourable fatigue performance, the role of the above effects has to be analysed and understood. To achieve such undertaking it is essential to consider their interaction with other parameters such as the nature of the target material and the loading conditions.

This work brings together two micromechanical models; one for notch sensitivity [5] and for fatigue life [6]. The former assesses the effect of surface roughening, whilst the latter incorporates the residual stress distribution and work hardening on fatigue life calculations. Combination of the two models allows the determination of the residual stress distribution to meet specific improvements in fatigue life (improvement life factor, ILF). Using the ILF methodology, the effects of CSP can be scrutinised against the stress level, the surface roughness and the ILF value.

Modelling the Surface Roughness

On shot peened surfaces, cracks are likely to form at micro-

notches (dents). Early studies from Smith [7] and Tanaka [8] indicate that the propagation of cracks from notches depends on the bluntness of the notch, given by $\sqrt{\beta/\rho}$ (ρ is the notch radius). Despite the numerous models published in the literature, an extended citation is given in [9], most models fail to provide a relationship between the geometry of the notch and the microstructure of the material. Such relationship was successfully provided by Vallellano et al [5,10]. According to their work, the nominal stress in a notched member is given by,

$$\sigma_i^{nom} = \frac{\sigma^{app}}{Z_i} \quad (1)$$

where σ^{app} is the applied stress, σ_i^{nom} is the distribution of the nominal stress ahead of the notch root as a function of the distance from the notch i , mapped as $i=2a/D$, and Z_i is the notch factor given by,

$$Z_i = \frac{\sqrt{i}}{\alpha + \beta} \left[\frac{\bar{\beta}}{\lambda_i} + \frac{\bar{\alpha}}{\sqrt{1 + \lambda_i^2}} \right]^{1/2}$$

$$\lambda_i = \frac{1}{\alpha^2 - \beta^2} \left[\alpha \sqrt{(\alpha + iD/2)^2 - \alpha^2 + \beta^2} - \beta (\alpha + iD/2) \right] \quad (2)$$

where $i=1,3,5,\dots$

The parameters $\bar{\alpha} = \frac{2\alpha}{D}$ and $\bar{\beta} = \frac{2\beta}{D}$ represent in a dimensionless form the notch depth α and the notch half width β . The parameter D represents the distance between two successive barriers. In the case where grain boundaries are considered being the dominant barrier, D is regarded as the grain diameter.

Li et al [11], proposed that the elastic stress concentration K_t introduced by multiple micro-notches in CSP, is somehow lower than the one determined in the case of a single notch of similar depth and width. The above finding reflects the uniformity of the micro-notches on the surface. According to Li, the resulting K_t from CSP is given by,

$$K_t = 1 + 2.1 \left(\frac{R_t}{S} \right) \tag{3}$$

where the parameters R_t and S are respectively the mean of peak-to-valley heights and the mean spacing of adjacent peaks in the surface roughness profile. In the case of a semi-elliptical notch and a high degree of uniformity (CSP coverage percentage of more than 100%), Eq.(3) can be written as,

$$K_t = 1 + 2.1 \left(\frac{\alpha}{2\beta} \right) \tag{4}$$

At the beginning of this section it was pointed out that the bluntness of the notch can significantly affect the strain generated at the root of the notch and consequently the propagation rate of the crack. In light of that, Smith and Miller [7] proposed that K_t should be determined by,

$$K_t = 1 + 2 \sqrt{\frac{\alpha}{\rho}} \tag{5}$$

where ρ is the notch root radius. In the case of a semi-elliptical notch, the notch root radius can be approximated by

$$\rho = \frac{\alpha^2}{\gamma} \text{ and thus Eq.(5) can be rewritten as,}$$

$$K_t = 1 + 2 \sqrt{\frac{\gamma}{\alpha}} \tag{6}$$

where α is the notch half width that considers the bluntness of the notch. By equating Eq.(6) with Eq.(4), the stress concentration due to multiple micro-notches can be expressed in terms of a single notch by,

$$K_t = 1 + \frac{\alpha}{\beta} \tag{7}$$

Modelling the Fatigue Life in CSP Components

In [4,6] it was proposed that the fatigue life of polycrystalline materials can be determined by,

$$N = \frac{1}{A_2} \sum_{i=1}^{i_c} \int_{n_s^i}^{n_c^i} \frac{\left(\frac{iD}{2} \right)^{1-m_2} dn_1^i}{CTOD^{m_2}} \tag{8}$$

where A_2, m_2 are parameters from the Paris law of crack propagation, CTOD is the crack tip opening displacement and n_s^i, n_c^i are limit values of n_1 as defined in Figure 1.

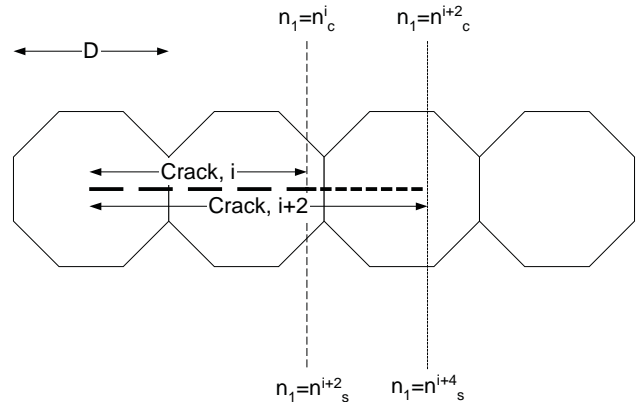


Figure 1. Schematic showing the position of n_1 prior (n_c) and after (n_s) the unblocking of the crack tip plasticity.

In Eq.(8) the parameter n_s^i and n_c^i represent respectively, the position of the crack tip at the beginning and end of each interval i of crack growth. These two parameters are calculated by,

$$n_c^i = \cos \left(\frac{\pi}{2} \frac{\sigma - \sigma_{i\ arrest}^p}{\sigma_2} \right) \tag{9}$$

$$n_s^i = n_c^{i-2} \frac{i-2}{i}$$

where σ_2 is the flow resistance of the material and $\sigma_{i\ arrest}^p$ is the Kitagawa-Takahashi formula for a plain specimen,

$$\sigma_{i\ arrest}^p = \frac{m_i}{m_1} \frac{\sigma_{FL}}{\sqrt{i}} \tag{10}$$

with σ_{FL} denoting the fatigue limit of the plain material. In Equation 10 the parameter m_i/m_1 represents the effect of the grain orientation factor. More details can be found in [4,12].

From Eq.(8) it is clear that the number of cycles required by the crack to propagate an i number of half grains, depends solely on the parameter n_c^i . For CSP components, the parameter n_c^i has to be modified in a way that it would take into account the roughening of the surface and the crack closure stresses generated by the residual stresses,

$$n_c^{i,CSP} = \cos \left(\frac{\pi}{2} \frac{\frac{\sigma}{Z_i} - \sigma_{i\ arrest}^{CSP}}{\sigma_2 - \sigma_1^i} \right) \tag{11}$$

where the parameter Z_i is taken by Equation 2. The Kitagawa-

Takahashi formula for the case of CSP, σ_i^{CSP} , is given by [4],

$$\sigma_i^{CSP} = \left(\frac{m_i}{m_1} \frac{\sigma_{FL}^{CSP} - \sigma_1^{i=1}}{\sqrt{i}} + \sigma_1^i \right) Z_i \quad (12)$$

where $\sigma_{FL}^{CSP} = \sigma_{FL} + \sigma_1^{i=1}$. Hence, Equation 12 is rewritten as,

$$\sigma_i^{CSP} = \left(\frac{m_i}{m_1} \frac{\sigma_{FL}}{\sqrt{i}} + \sigma_1^i \right) Z_i \quad (13)$$

Introducing the Improvement Life Factor (ILF)

In order to increase the life consumed at each grain and consequently the overall life of the CSP component, we make use of a predetermined ILF,

$$ILF \times N = \frac{1}{A_2} \int_{n_c^{i,CSP}}^{n_s^{i,CSP}} \left(\frac{id}{2} \right)^{1-m_2} \frac{dn_i^{i,CSP}}{CTOD^{m_2}} \quad (14)$$

where the values of ILF are in percentage. Solution of Equation 14 in terms of CTOD yields,

$$\ln(CTOD) = \frac{0.69(m_2 - 1)}{m_2} + \frac{\ln \left[\frac{(n_c^{i,CSP} - n_s^{i,CSP})(Di)^{(1-m_2)}}{A_2 \times ILF \times N} \right]}{m_2} \quad (15)$$

In the case of a plain/unpeened material, Equation 15 is written as,

$$\ln(CTOD) = \frac{0.69(m_2 - 1)}{m_2} + \frac{\ln \left[\frac{(n_c^{i,p} - n_s^{i,p})(Di)^{(1-m_2)}}{A_2 N} \right]}{m_2} \quad (16)$$

The fact that the value of CTOD at the position n_c , where the crack tip plasticity is able to overcome the microstructural barrier, is identical for both the peened and the unpeened material (for the same loading conditions) allows Equations 15, 16 to be equated,

$$\frac{0.69(m_2 - 1)}{m_2} + \frac{\ln \left[\frac{(n_c^{i,CSP} - n_s^{i,CSP})(Di)^{(1-m_2)}}{A_2 \times ILF \times N} \right]}{m_2} = \frac{0.69(m_2 - 1)}{m_2} + \frac{\ln \left[\frac{(n_c^{i,p} - n_s^{i,p})(Di)^{(1-m_2)}}{A_2 N} \right]}{m_2} \quad (17)$$

Simplification of Equation 17 gives,

$$n_c^{i,CSP} = ILF \times (n_c^{i,p} - n_s^{i,p}) + n_s^{i,CSP} \quad (18)$$

From Equation 18, the closure stress σ_i^i can be determined. It should

be noted that due to the complexity of Equation 18, a computational solution is advised. Figure 2 shows the calculated crack closure, σ_i^i , for several conditions of loading and treatment.

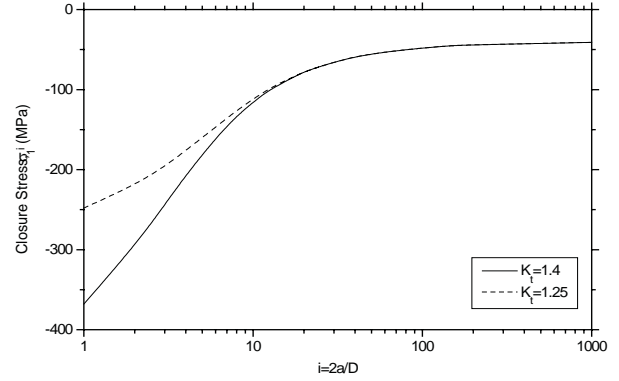


Figure 2a. The effect of surface roughness on the distribution of closure stress in a 2024-T351 CSP component under mode I loading. The parameters used in the calculations are: ILF=5%, $\sigma = 350$ MPa, $\sigma_2 = 450$ MPa, $\sigma_{FL} = 220$ MPa and $D = 52 \mu\text{m}$. Converging of the two distributions at around the 15th half grain is due to the small difference between the selected K_t values and should not be generalised.

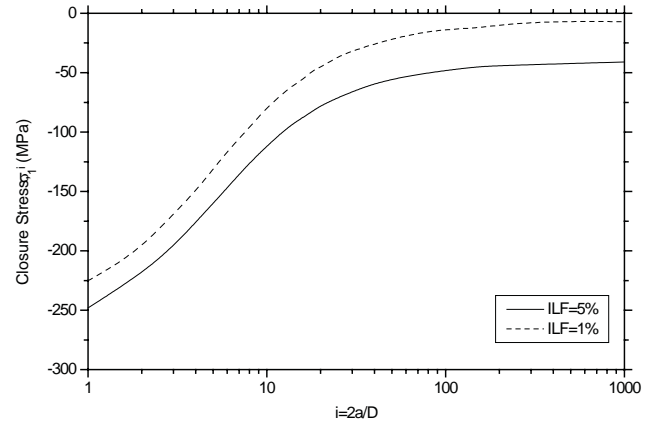


Figure 2b. The effect of ILF on the distribution of closure stress in a 2024-T351 CSP component under mode I loading. The parameters used in the calculations are: $K_t = 1.25$, $\sigma = 350$ MPa, $\sigma_2 = 450$ MPa, $\sigma_{FL} = 220$ MPa and $D = 52 \mu\text{m}$. The scale difference of the closure stress distribution between the short (<10 half grains) and long crack (>10 half grains) regions signifies the experimentally proven tendency of short cracks to be less affected by closure phenomena.

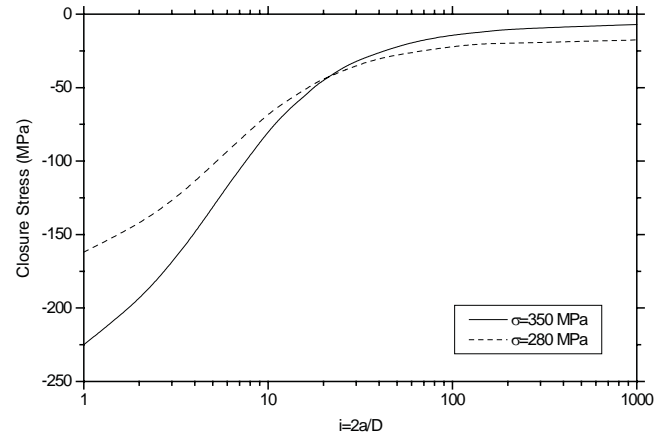


Figure 2c. The effect of the far-field stress on the distribution of closure stress in a 2024-T351 CSP component under mode I loading. The parameters used are: $K_t = 1.25$, ILF=1%, $\sigma_2 = 450$ MPa, $\sigma_{FL} = 220$ MPa and $D = 52 \mu\text{m}$. The difference in the decay rate of the distributions reflects the fact that a high

far-field stress level will reduce faster the influence of the stress raiser. This should not be taken as beneficial since high far-field stress level will increase the premature initiation of a "visible" crack.

Discussion and Conclusions

In this work the effects of CSP are analysed and modelled according to their effects on fatigue damage. Surface roughness is modelled in a way that would increase the far-field stress. Hence, the component appears having an amplified capacity of initiating and propagating short fatigue cracks. Compressive residual stresses translated as closure stresses are regarded as one of the beneficial effect of CSP. Residual stresses tend to reduce the application of the far-field stress by introducing a closure stress on the crack flanks. Thus, the propagation of the crack is expected to be somewhat reduced compared to the unpeened condition. Finally, strain hardening is expected to reduce the propagation of short fatigue cracks by increasing the ability of the material to localised straining (crack tip plastic zone).

The introduction of a predetermine improvement in terms of fatigue life (ILF) has been achieved by introducing the ILF into the number of fatigue cycles consumed in every grain. The above approach allows the mathematical modelling of the conflict between the beneficial and detrimental CSP effects. At first the analysis reveals that the magnitude of the closure stresses should always attain a maximum at the surface. Such distribution minimises the premature initiation of a "visible" fatigue crack. Secondly, the depth distribution should be able to follow the stress gradient generated by the surface roughness. Further analysis allows to scrutinise against parameters like the far-field stress level, the ILF and the surface roughness. From Figure 2, the effect of the above parameter is classified in the following order, starting from the most decisive: a) Surface Roughness. The analysis reveals that a 12% increase, measured in terms of K_t , in the surface roughness requires a 47% increase in the closure stress magnitude to allow a 5% increase in the per grain life. Additionally, a higher K_t would require deeper closure stresses; b) Far-Field Stress Level. In principle high far-field stress levels require high magnitude and deeper closure stresses. This comes as a verification to the fact, published extensively in the literature, that CSP will have a minimum effect, or in some cases a detrimental effect, on

the low cycle fatigue region; and c) ILF. The analysis reveals that CSP components are not so sensitive to different ILF values. The above finding is in accordance to many experimental data where short cracks were found to propagate almost irrespective of the crack closure stress levels.

It should be noted that due to the fact that the methodology is expressed in terms of crack length, it can be easily adjusted to incorporate relaxation profiles of residual stress and strain hardening.

References

- [1] P. O'Hara in Surface Treatment IV, (Ed. . Brebbia and J. M. Kenny) WIT Press, 321-330. 1999.
- [2] L. Wagner and G. Lütjering in Shot Peening, Pergamon press, 453-460. 1981.
- [3] P. K. Sharp and G. Clark DSTO-RR-0208, Defence-Science and Technology Organisation, Royal Australian Air Force, Australian Ministry of Defence, (declassified). 2001.
- [4] S. Curtis, E. R. de los Rios, C. A. Rodopoulos, A. Levers, Inter. J. of Fatigue, Volume 25, Issue 1, pp. 59-66. 2003.
- [5] C. Vallellano, A. Navarro and J. Domínguez, Fatigue Fracture Engineering Materials Structures, 23, 113-121. 2000.
- [6] E. R. de los Rios, M. Trull and A. Levers, Fatigue Fracture Engineering Materials Structures, 23, 709-716. 2000.
- [7] R. A. Smith and K. J. Miller, Inter. J. Mech. Sci., 20, 201-206. 1978.
- [8] K. Tanaka, Inter. J. Fract., 22, R39-R45. 1983.
- [9] S. Suresh, Fatigue of Materials, Cambridge University Press, 1991.
- [10] C. Vallellano, A. Navarro and J. Domínguez, Fatigue Fracture Engineering Materials Structures, 2000, 23, 123-128.
- [11] J. K. Li, M. Yao, D. Wang., R. Wang, Fatigue Fracture Engineering Materials Structures, 1999, 15(12), 1271 - 1279.
- [12] E. R. de los Rios and A. Navarro, (1990) Philosophical Magazine 1990, 61, 435-449.